

RADAMS: Resilient and Adaptive Alert and Attention Management Strategy against Informational Denial-of-Service (IDoS) Attacks

Linan Huang, *Student Member, IEEE*, and Quanyan Zhu, *Senior Member, IEEE*

Abstract—Attacks exploiting human attentional vulnerability have posed severe threats to cybersecurity. In this work, we identify and formally define a new type of proactive attentional attacks called Informational Denial-of-Service (IDoS) attacks that generate a large volume of feint attacks to overload human operators and hide real attacks among feints. We incorporate human factors (e.g., levels of expertise, stress, and efficiency) and empirical results (e.g., the Yerkes–Dodson law and the sunk cost fallacy) to model the operators’ attention dynamics and their decision-making processes along with the real-time alert monitoring and inspection. To assist human operators in timely and accurately dismissing the feints and escalating the real attacks, we develop a Resilient and Adaptive Data-driven alert and Attention Management Strategy (RADAMS) that deemphasizes alerts selectively based on the alerts’ observable features. RADAMS uses reinforcement learning to achieve a customized and transferable design for various human operators and evolving IDoS attacks. The integrated modeling and theoretical analysis lead to the Product Principle of Attention (PPoA), fundamental limits, and the tradeoff among crucial human and economic factors. Experimental results corroborate that the proposed strategy outperforms the default strategy and can reduce the IDoS risk by as much as 20%. Besides, the strategy is resilient to large variations of costs, attack frequencies, and human attention capacities. We have recognized interesting phenomena such as attentional risk equivalency, attacker’s dilemma, and the half-truth optimal attack strategy.

Index Terms—Human attention vulnerability, feint attacks, reinforcement learning, risk analysis, cognitive load, alert fatigue.

I. INTRODUCTION

HUMAN vulnerability and human-induced security threats have been a long-standing and fast-growing problem for the security of Industrial Control Systems (ICSs). According to Verizon [2], 85% data breach involves human errors. Attentional vulnerability is one of the representative human vulnerabilities. Adversaries have exploited human inattention to launch social engineering attacks and phishing attacks toward employees and users. According to the report [3], 29% of employees fall for a phishing scam and 36% of employees send a misdirected email owing to lack of attention. These attentional attacks are *reactive* as they exploit the existing human attention patterns. On the contrary, *proactive* attentional attacks can strategically change the attention pattern of a

L. Huang and Q. Zhu are with the Department of Electrical and Computer Engineering, New York University, Brooklyn, NY, 11201, USA. E-mail: {lh2328, qz494}@nyu.edu

A preliminary version of this work [1] was presented at the 12th Conference on Decision and Game Theory for Security.

human operator or a network administrator. For example, an attacker can launch feint attacks to trigger a large volume of alerts and overload the human operators so that operators fail to inspect the alert associated with real attacks [4]. We refer to this new type of attacks as the Informational Denial-of-Service (IDoS) attacks, which aim to deplete the limited attention resources of human operators to prevent them from accurate detection and timely defense.

IDoS attacks bring significant security challenges to ICSs for the following reasons. First, alert fatigue has already been a serious problem in the age of infobesity with terabytes of unprocessed data or manipulated information. IDoS attacks exacerbate the problem by generating feints to intentionally increase the percentage of false-positive alerts. Second, IDoS attacks directly target the human operators and security analysts in the Security Operations Center (SOC). Third, as ICSs become increasingly complicated and time-critical, the human operators require higher expertise levels to understand the domain information and detect feints. Finally, since human operators behave differently and IDoS attacks are a broad class of adaptive attacks, it is challenging (yet highly desirable) to develop a customized and resilient defense. There is an apparent need to understand this class of proactive attentional attacks, quantify its consequences and risks, and develop associated mitigation strategies.

To this end, we establish a holistic model of IDoS attacks, alert generations, and the human operators’ monitoring, inspections, and decision-making of alerts. In the IDoS attack model, we adopt a Markov renewal process to characterize the sequential arrival of feints and real attacks that target different ICS components. We use revelation probability to abstract the alert generation and triage process of existing detection systems. The revelation probability maps the attacks’ hidden types and targets stochastically to the associated alerts’ observable category labels. To model the human operators’ attention dynamics and alert responses under the IDoS attacks, we directly incorporate the operators’ levels of expertise, stress, and efficiency into the security design based on the existing results from the literature in psychology, including the Yerkes–Dodson law [5] and the sunk cost fallacy [6]. To assist human operators in alert inspection and response, compensate for their attentional vulnerabilities, and combat IDoS attacks, we develop human-centered technologies that selectively make some alerts less noticeable based on their category labels. Reinforcement learning is applied to make the human-assistive security technology *resilient, automatic,*

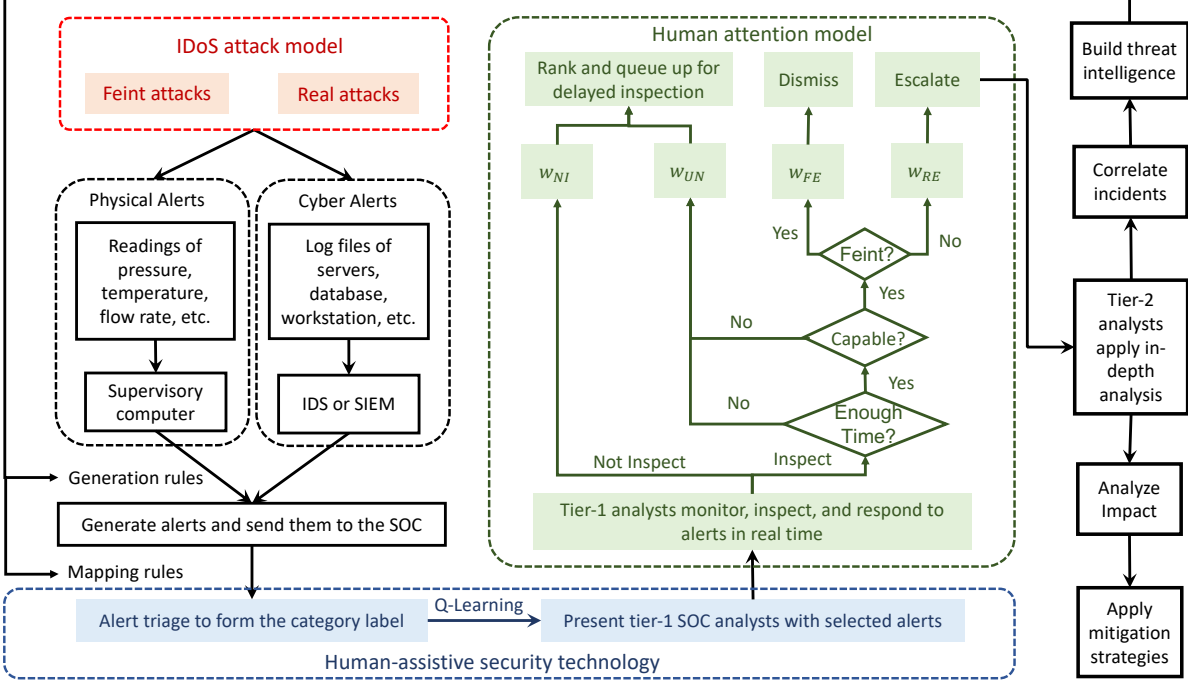


Fig. 1: The overview diagram of RADAMS against IDoS in ICS, which incorporates the IDoS attack model, human attention model, and the human-assistive security technology in the red, green, and blue boxes, respectively. The processes in black are not the focus of this work. The modern SOC adopts a hierarchical alert analysis process. The tier-1 SOC analysts, also referred to as the operators, are in charge of real-time alert monitoring and inspections. The tier-2 SOC analysts are in charge of the in-depth analysis.

and *adaptive* to various human models and attack scenarios.

We illustrate the overview diagram of Resilient and Adaptive Alert and Attention Management Strategy (RADAMS) in Fig. 1. RADAMS enriches the existing alert selection frameworks with the IDoS attack model, the human attention model, and the human-assistive security technology highlighted in red, green, and blue, respectively. Through the integrated modeling and theoretical analysis, we obtain the *Product Principle of Attention* (PPoA), which states that the Attentional Deficiency Level (ADL), i.e., the probability of incomplete alert responses, and the risk of IDoS attacks depend on the product of the supply and the demand of human attention resources. The closed-form expressions under mild assumptions lead to several fundamental limits, including the minimum ADL and the maximum length of de-emphasized alerts to reduce IDoS risk. We explicitly characterize the tradeoff among crucial factors such as the ADL, the reward of alert attention, and the impact of alert inattention.

Finally, we propose an algorithm to learn the adaptive AM strategy based on the operator's alert inspection outcomes. We present several case studies based on the simulation of different IDoS attacks and alert inspecting processes. The numerical results show that the proposed optimal AM strategy outperforms the default strategy and can effectively reduce the IDoS risk by as much as 20%. The strategy is also resilient to a large range of cost variations, attack frequencies, and human attention capacities. We have observed the phenomenon of *attentional risk equivalency*, which states that the deviation from the optimal to sub-optimal strategies for some category labels can reduce the risk under the default strategy to approximately

the same level. The results also corroborate that RADAMS can adapt to different category labels to strike a balance of quantity (i.e., inspect more alerts) and quality (i.e., complete alert responses to dismiss feints and escalate real attacks). Finally, we identify the *attacker's dilemma* where destructive IDoS attacks induce unbearable costs to the attacker. We also identify the *half-truth attack strategy* as the optimal IDoS attack strategy when feints are generated at a high cost.

A. Organization of the Paper

The rest of the paper is organized as follows. The related works are presented in Section II. Sections IV, IV, and V introduce the IDoS attack model, the human operator model, and the human-assistive security technology, respectively. We analyze the attentional deficiency level and the risk of IDoS attacks in closed form for the class of ambitious operators in Section VI. Section VII presents a case study of alert inspection under IDoS attacks and adaptive AM strategies. Section VIII concludes the paper.

II. RELATED WORKS

A. Alert Management

Previous works have applied alert management methods during the alert generation, detection, and response processes to mitigate alert fatigue and enhance cybersecurity.

1) *Source Management:* On the one hand, proactive defense [7] and deception techniques, including honeypots [8], [9] and moving target defense [10], have managed to reduce successful attacks and the resulting alerts from the source.

On the other hand, previous works have designed incentive mechanisms (e.g., [11], [12]) and information mechanisms (e.g., [13]) to enhance insiders' compliance, reduce users' misbehavior, and reduce false positives.

2) *Detection Management*: A rich literature has attempted to develop detection systems capable of reducing false positives while maintaining the ability to detect malicious behaviors. Methods include statistical analysis [14], fuzzy inference [15], and machine learning approaches [16]. Alert aggregation and correlation methods [17] have also been applied to dismiss repeated and innocuous alerts and generate alerts of system-level threat information.

3) *Response Management*: Despite the significant advances of alert reduction methods introduced in Section II-A1 and II-A2, the demand for alert inspection still exceeds the operators' capacity. To this end, researchers have developed alert selection and prioritization approaches through simulated-based optimization [18], fuzzy logic [19], deep learning [20], and reinforcement learning [21]. Compared to the works that rank the alerts based on their contextual information, our human-centered approach explicitly models the attentional behaviors of human operators and selects alerts based on human cognitive capacity.

B. Feint Attacks and Human Attentional Models

There is a rich literature on attacks against detection systems [22]. In particular, the authors in [23], [24] have developed tools that can generate false positives by matching detection signatures. The tools are tested on SNORT [25] and the empirical results verify the feasibility of feint attacks on detection systems. Different from the practical feint attacks that focus on the vulnerability of detection systems, we focus on the attentional vulnerabilities and the impact of feints on human operators. Moreover, we abstract models to formally characterize general feint attacks, enabling us to quantify the risk and develop human-assistive security technologies.

We can classify human vulnerabilities into acquired vulnerabilities (e.g., lack of security awareness and noncompliance) and innate ones (e.g., bounded attention and rationality) based on whether they can be mitigated through short-term training and security rules. Many works (e.g., [11], [13], [26]) have emphasized the urgency and necessity to reduce acquired human vulnerability and proposed human-assistive strategies. However, few works have focused on mitigation strategies for innate vulnerabilities. Visual support systems have been used for rapid cyber event triage [27] and alert investigations [28], and eye-tracking data have been incorporated to enhance attention for phishing identification [29]. The authors in [30] perform an anthropological study in a corporate SOC to model and mitigate security analyst burnout. These works lay the foundations of empirical solutions to mitigate human attentional vulnerabilities. Our work combines real-time human behavioral and decision data with the well-identified human factors to enable quantitative characterizations of the empirical relationship such as the Yerkes–Dodson law [5]. The learning-based method for attention handling also makes our human-assistive technology adaptive and transferable to various human-technical systems.

III. IDOS ATTACKS AND SEQUENTIAL ALERT ARRIVALS

As illustrated in the first column of Fig. 1, after the IDoS attacker has generated feint and real attacks, the detection system monitors the readings from physical layers and log files from cyber layers and generates alerts according to the *generation rules*. Then, the alerts are sent to the SOC and a triage system automatically generates their category labels (e.g., the alerts' criticality) based on the *mapping rules*. The rules for alert generation and triage mapping are pre-defined and their designs are not the focus of this work.

A. Feint and Real Attacks of Heterogeneous Targets

After the initial intrusion, privilege escalation, and lateral movement, IDoS attackers can launch feint and real attacks sequentially as illustrated by the solid red arrows in Fig. 2. With a deliberate goal of triggering alerts, feint attacks require fewer resources to craft. Although feints have limited impacts on the target system, they aggravate the alert fatigue by depleting human attention resources and preventing human operators from a timely response to real attacks. For example, the attacker can attempt to access a database with wrong credentials intentionally, and in the meantime, gradually changes the temperature of the reactor of a nuclear power plant. The repeated log-in attempts trigger an excessive number of alerts so that the overloaded human operators fail to pay sustained attention and respond timely to the sensor alerts of the temperature deviation.

We denote feint and real attacks as θ_{FE} and θ_{RE} , respectively, where $\Theta := \{\theta_{FE}, \theta_{RE}\}$ is the set of attacks' types. Each feint or real attack can target cyber components (e.g., servers, databases, and workstations) or physical components (e.g., sensors of pressure, temperature, and flow rate) in the ICS. We define Φ as the set of the potential attack targets. The stochastic arrival of these attacks is modeled as a Markov renewal process where $t^k, k \in \mathbb{Z}^{0+}$, is the time of the k -th arrival. We refer to the k -th attack equivalently as the attack at *attack stage* $k \in \mathbb{Z}^{0+}$ and let $\theta^k \in \Theta$ and $\phi^k \in \Phi$ be the attack's type and target at attack stage $k \in \mathbb{Z}^{0+}$, respectively. Define $\kappa_{AT} \in \mathcal{K}_{AT} : \Theta \times \Phi \times \Theta \times \Phi \mapsto [0, 1]$ as the transition kernel where $\kappa_{AT}(\theta^{k+1}, \phi^{k+1} | \theta^k, \phi^k)$ denotes the probability that the $(k+1)$ -th attack has type $\theta^{k+1} \in \Theta$ and target $\phi^{k+1} \in \Phi$ when the k -th attack has type $\theta^k \in \Theta$ and target $\phi^k \in \Phi$. The inter-arrival time $\tau^k := t^{k+1} - t^k$ is a continuous random variable with support $[0, \infty)$ and Probability Density Function (PDF) $z \in \mathcal{Z} : \Theta \times \Phi \times \Theta \times \Phi \mapsto \mathbb{R}^{0+}$ where $z(t | \theta^{k+1}, \phi^{k+1}, \theta^k, \phi^k)$ is the probability that the inter-arrival time is t when the attacks' types and targets at attack stage k and $k+1$ are θ^k, ϕ^k and θ^{k+1}, ϕ^{k+1} , respectively. The values of $\kappa_{AT} \in \mathcal{K}_{AT}$ and $z \in \mathcal{Z}$ are unknown to human operators and the designer of RADAMS. Attackers can adapt κ_{AT} and z to different ICS and alert inspection schemes to achieve the attack goals. We formally define IDoS attacks in Definition 1.

Definition 1 (IDoS Attacks). *An IDoS attack is a sequence of feint and real attacks of heterogeneous targets, which can be characterized by the 4-tuple $(\Theta, \Phi, \mathcal{K}_{AT}, \mathcal{Z})$.*

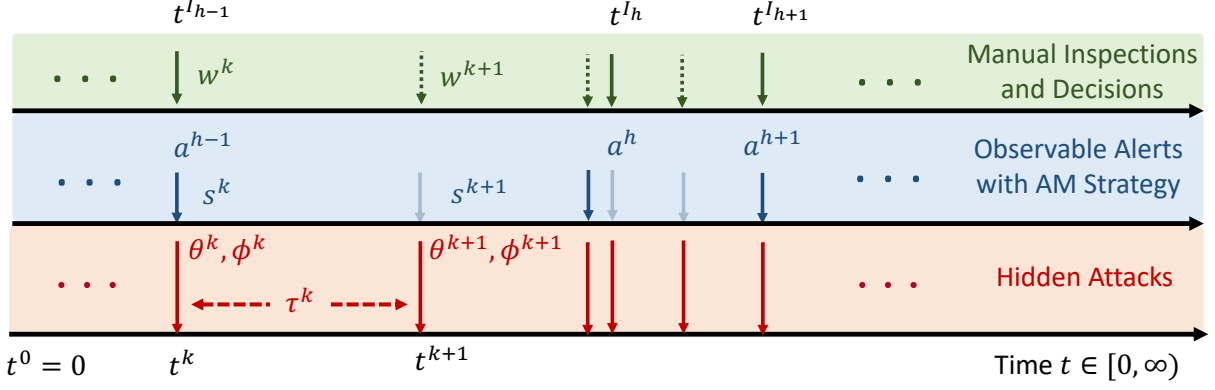


Fig. 2: The timelines of an IDoS attack, alerts under AM strategies, and manual inspections are depicted in red, blue, and green, respectively. The inspection stage $h \in \mathbb{Z}^{0+}$ is equivalent to the attack stage $I_h \in \mathbb{Z}^{0+}$. The red arrows represent the sequential arrivals of feints and real attacks. The semi-transparent blue the dashed green arrows represent the de-emphasized alerts and the alerts without inspections, respectively.

B. Alert Triage Process and System-Level Metrics

The alerts triggered by IDoS attacks contain *device-level* contextual information, including the software version, hardware parameters, existing vulnerabilities, and security patches. The alert triage process consists of rules that map the device-level information to the *system-level* metrics, which helps human operators make timely responses. Some essential metrics are listed as follows.

- **Source** $s_{SO} \in \mathcal{S}_{SO}$: The ICS sensors or the cyber components that the alerts are associated with.
- **Time Sensitivity** $s_{TS} \in \mathcal{S}_{TS}$: The length of time that the potential attack needs to achieve its attack goals.
- **Complexity** $s_{CO} \in \mathcal{S}_{CO}$: The degree of effort that a human operator takes to inspect the alert.
- **Susceptibility** $s_{SU} \in \mathcal{S}_{SU}$: The likelihood that the attack succeeds and inflicts damage on the protected system.
- **Criticality** $s_{CR} \in \mathcal{S}_{CR}$: The consequence or the impact of the attack's damage.

These alert metrics are observable to the human operator and the RADAMS designer, and they form the *category label* of an alert. We define the category label associated with the k -th alert as $s^k := (s_{SO}^k, s_{TS}^k, s_{CO}^k, s_{SU}^k, s_{CR}^k) \in \mathcal{S}$ where $\mathcal{S} := \mathcal{S}_{SO} \times \mathcal{S}_{TS} \times \mathcal{S}_{CO} \times \mathcal{S}_{SU} \times \mathcal{S}_{CR}$. The joint set \mathcal{S} can be adapted to suit the organization's security practice. For example, we have $\mathcal{S}_{TS} = \emptyset$ if time sensitivity is unavailable or unimportant.

The alert triage process establishes a stochastic connection between the hidden types and targets of IDoS attacks and the observable category labels of the associated alerts. Let $o(s^k | \theta^k, \phi^k)$ be the probability of obtaining category label $s^k \in \mathcal{S}$ when the associated attack has type $\theta^k \in \Theta$ and target $\phi^k \in \Phi$. The revelation kernel o reflects the quality of the alert triage. For example, feints with lightweight resource consumption usually have a limited impact. Thus, a high-quality triage process should classify the associated alert as low criticality with a high probability. Letting $b(\theta^k, \phi^k)$ denote the probability that the k -th attack has type θ^k and target ϕ^k at the steady-state, we can compute the steady-state distribution b in closed form based on κ_{AT} . Then, the transition of category labels at different attack stages is also Markov

and is represented by $\kappa_{CL} \in \mathcal{K}_{CL} : \mathcal{S} \times \mathcal{S} \mapsto [0, 1]$. We can compute $\kappa_{CL} = \frac{\Pr(s^{k+1}, s^k)}{\sum_{s^{k+1} \in \mathcal{S}} \Pr(s^{k+1}, s^k)}$ based on κ_{AT}, o, b , where $\Pr(s^{k+1}, s^k) = \sum_{\theta^k, \theta^{k+1} \in \Theta} \sum_{\phi^k, \phi^{k+1} \in \Phi} \kappa_{AT}(\theta^{k+1}, \phi^{k+1} | \theta^k, \phi^k) o(s^k | \theta^k, \phi^k) o(s^{k+1} | \theta^{k+1}, \phi^{k+1}) b(\theta^k, \phi^k)$. In this work, we focus on the case where the detection system introduces the same delay between attacks and their triggered alerts. Since the sequences of attacks and alerts have a one-to-one mapping, we can consider zero delay time without loss of generality. Hence, the sequence of alerts associated with an IDoS attack $(\Theta, \Phi, \mathcal{K}_{AT}, \mathcal{L})$ is also a Markov renewal process characterized by the 3-tuple $(\mathcal{S}, \mathcal{K}_{CL}, \mathcal{L})$.

IV. HUMAN ATTENTION MODEL UNDER IDOS ATTACKS

An SOC typically adopts a hierarchical alert analysis [31]. The attention model in this section applies to the tier-1 SOC analysts, or the operators, who are in charge of monitoring, inspecting, and responding to alerts in real time. As illustrated by the green box in Fig. 1, the operators choose to inspect certain alerts, dismiss the feints, and escalate the real attacks to tier-2 SOC analysts for in-depth analysis. The in-depth analysis can last hours to months, during which the tier-2 analysts correlate incidents from different components in the ICS over long periods to build threat intelligence and analyze the impact. The threat intelligence is then incorporated to form and update the generation rules of the detection system and mapping rules of the triage process.

A. Alert Responses

Due to the high volume of alerts and the potential short-term surge arrivals, human operators cannot inspect all alerts in real time. The uninspected alerts receive an alert response w_{NI} . Whether the operator chooses to inspect an alert depends on the switching probability in Section IV-B.

When the operator inspects an alert, he can be distracted by the arrival of new alerts and switch to newly-arrived alerts without completing the current inspection. We elaborate on the attention dynamics in Section IV-C. The alert with incomplete inspection is labeled by w_{UN} . Besides the insufficient

inspection time, the operator's cognitive capacity constraint can also prevent him from determining whether the alert is triggered by a feint or a real attack. In this work, we consider prudent operators. When they cannot determine the attack's type after a full inspection, the associated alert is labeled as w_{UN} . We elaborate on how the insufficient inspection time and the operator's cognitive capacity constraint lead to w_{UN} , i.e., referred to as the *inadequate alert response*, in Section IV-D. The alerts labeled as w_{NI} and w_{UN} are ranked and queued up for delayed inspections at later stages.

When the operator successfully completes the alert inspection with a deterministic decision, he either dismisses the alert (denoted by w_{FE}) or escalates the alert to tier-2 SOC analysts for in-depth analysis (denoted by w_{RE}) as shown in Fig. 1. We use $w^k \in \mathcal{W} := \{w_{FE}, w_{RE}, w_{UN}, w_{NI}\}$ to denote the operator's response to the alert at attack stage $k \in \mathbb{Z}^{0+}$. We can extend the set \mathcal{W} to suit the organization's security practice. For example, some organizations let the operators report their estimations and confidence levels concerning incomplete alert inspection, i.e., divide the label w_{UN} into finer subcategories. At later stages, the delayed inspection prioritizes the alerts estimated to be associated with real attacks of high confidence levels.

B. Probabilistic Switches within Allowable Delay

Alerts are monitored in real time when they arrive. When the category label of the new alert indicates higher time sensitivity, susceptibility, or criticality, the operator can delay the current inspection (i.e., label the alert under inspection as w_{UN}) and switch to inspect the new alert. We denote $\kappa_{SW}^{\Delta k}(s^{k+\Delta k} | s^k)$ as the operator's switching probability when the previous alert at attack stage k and the new alert at stage $k + \Delta k, \Delta k \in \mathbb{Z}^+$, have category label $s^k \in \mathcal{S}$ and $s^{k+\Delta k} \in \mathcal{S}$, respectively. As a probability measure,

$$\sum_{\Delta k=1}^{\infty} \sum_{s^{k+\Delta k} \in \mathcal{S}} \kappa_{SW}^{\Delta k}(s^{k+\Delta k} | s^k) \equiv 1, \forall k \in \mathbb{Z}^{0+}, \forall s^k \in \mathcal{S}. \quad (1)$$

Since the operator cannot observe the attack's hidden type and hidden target, the switching probability $\kappa_{SW}^{\Delta k}$ is independent of θ^k, ϕ^k and θ^{k+1}, ϕ^{k+1} . The switching probability depends on the time that the operator has already spent on the current inspection. For example, an operator becomes less likely to switch after spending a long time inspecting an alert of low criticality or beyond his capacity, which can lead to the Sunk Cost Fallacy (SCF).

We denote $D_{max} \in \mathbb{R}^+$ as the Maximum Allowable Delay (MAD). At time $t \geq t^k$, the k -th alert's Age of Information (AoI) [32] is defined as $t_{AoI}^k := t - t^k$. This work focuses on time-critical ICSs where a defensive response for the k -th alert is only effective when the alert's AoI is within the MAD, i.e., $t_{AoI}^k \leq D_{max}$. Therefore, the operator will be reminded when an alert's AoI exceeds the MAD so that he can switch to monitor and inspect new alerts. The MAD and the reminder scheme help mitigate the SCF when the operators are occupied with old alerts and miss the chance to monitor and inspect new alerts in real time.

C. Attentional Factors

We identify the following human and environmental factors affecting operators' alert inspection and response processes.

- The operator's expertise level denoted by $y_{EL} \in \mathcal{Y}_{EL}$.
- The k -th alert's category label $s^k \in \mathcal{S}$.
- The k -th attack's type θ^k and target ϕ^k .
- The operator's stress level $y_{SL}^t \in \mathbb{R}^+$, which changes with time t as new alerts arrive.

The first three factors are the static attributes of the analyst, the alert, and the IDoS attack, respectively. They determine the average inspection time, denoted by $\bar{d}(y_{EL}, s^k, \theta^k, \phi^k) \in \mathbb{R}^+$, to reach a *complete response* w_{FE} or w_{RE} . For example, if the inspected alert is of low complexity, the operator can reach a complete response in a shorter time. Also, it takes a senior operator less time on average to reach a complete alert response than a junior one does. We use $d(y_{EL}, s^k, \theta^k, \phi^k)$ to represent the Actual Inspection Time Needed (AITN) when the operator is of expertise level y_{EL} , the alert is of category label s^k , and the attack has type θ^k and target ϕ^k . AITN $d(y_{EL}, s^k, \theta^k, \phi^k)$ is a random variable with mean $\bar{d}(y_{EL}, s^k, \theta^k, \phi^k)$.

The fourth factor reflects the temporal aspect of human attention during the inspection process. Evidence has shown that the continuous arrival of the alerts can increase the stress level of human operators [33] and 52% of employees attributes their mistakes to stress [3]. We denote $n^t \in \mathbb{Z}^{0+}$ as the number of alerts that arrive during the current inspection up to time $t \in [0, \infty)$ and model the operator's stress level y_{SL}^t as an increasing function f_{SL} of n^t , i.e., $y_{SL}^t = f_{SL}(n^t)$. At time $t \in [0, \infty)$, the human operator's Level of Operational Efficiency (LOE), denoted by $\omega^t \in [0, 1]$, is a function f_{LOE} of the stress level y_{SL}^t , i.e.,

$$\omega^t = f_{LOE}(y_{SL}^t) = (f_{LOE} \circ f_{SL})(n^t), \forall t \in [0, \infty). \quad (2)$$

Based on the Yerkes–Dodson law, the function f_{LOE} follows an inverse U-shape that contains the following two regions. In region one, a small number of alerts result in a moderate stress level and allow human operators to inspect the alert efficiently. In region two, the LOE starts to decrease when the number of alerts to inspect is beyond some threshold $\bar{n}(y_{EL}, s^k)$ and the human operator is overloaded. The value of the *attention threshold* $\bar{n}(y_{EL}, s^k)$ depends on the operator's expertise level $y_{EL} \in \mathcal{Y}_{EL}$ and the alert's category label $s^k \in \mathcal{S}$. For example, it requires more (resp. fewer) alerts (i.e., higher (resp. lower) attention threshold) to overload a senior (resp. an inexperienced) operator. We can also adapt the value of $\bar{n}(y_{EL}, s^k)$ to different scenarios. In the extreme case where all alerts are of high complexity and create a heavy cognitive load, we let $\bar{n}(y_{EL}, s^k) = 0, \forall y_{EL} \in \mathcal{Y}_{EL}, s^k \in \mathcal{S}$, and the LOE decreases monotonously with the number of alert arrivals during an inspection.

D. Alert Responses under Time and Capacity Limitations

After we identify attentional factors in Section IV-C, we illustrate their impacts on the operators' alert responses as follows. We define the Effective Inspection Time (EIT) during inspection time $[t_1, t_2]$ as the integration $\tilde{\omega}^{t_1, t_2} := \int_{t_1}^{t_2} \omega^t dt$. When the operator is overloaded and has a low LOE during

$[t_1, t_2]$, the EIT $\tilde{\omega}^{t_1, t_2}$ is much shorter than the actual inspection time $t_2 - t_1$.

Suppose that the operator of expertise level y_{EL} inspects the k -th alert for a duration of $[t_1, t_2]$. If the EIT has exceed the AITN $d(y_{EL}, s^k, \theta^k, \phi^k)$, then the operator can reach a complete response w_{FE} or w_{RE} with a high success probability denoted by $p_{SP}(y_{EL}, s^k, \theta^k, \phi^k) \in [0, 1]$. However, when $\tilde{\omega}^{t_1, t_2} < d(y_{EL}, s^k, \theta^k, \phi^k)$, it indicates that the operator has not completed the inspection and the alert response concerning the k -th alert is $w^k = w_{UN}$. The success probability p_{SP} depends on the operator's capacity to identify attacks' types, which leads to the definition of the capacity gap below.

Definition 2 (Capacity Gap). For an operator of expertise level $y_{EL} \in \mathcal{Y}_{EL}$, we define $p_{CG}(y_{EL}, s^k, \theta^k, \phi^k) := 1 - p_{SP}(y_{EL}, s^k, \theta^k, \phi^k)$ as his capacity gap to inspect an alert with category label $s^k \in \mathcal{S}$, type $\theta^k \in \Theta$, and target $\phi^k \in \Phi$ defined in Section III.

V. HUMAN-ASSISTIVE SECURITY TECHNOLOGY

As illustrated in Section IV, the frequent arrival of alerts triggered by IDoS attacks can overload the human operator and reduce the LOE and the EIT. To compensate for the human's attentional limitation, we can intentionally make some alerts less noticeable, e.g., without sounds or in a light color, based on their category labels. As illustrated by the blue box in Fig. 1, based on the category labels from the triage process, RADAMS automatically emphasizes and de-emphasizes alerts, and then presents them to the tier 1 SOC analysts.

A. Adaptive AM Strategy

In this work, we focus on the class of Attention Management (AM) strategies, denoted by $\mathcal{A} := \{a_m\}_{m \in \{0, 1, \dots, M\}}$, that de-emphasize consecutive alerts. As explained in Section IV-A, the operator can only inspect some alerts in real time. Thus, we use $I_h \in \mathbb{Z}^{0+}$ and $t^h \in [0, \infty)$ to denote the index and the time of the alert under the h -th inspection; i.e., the inspection stage $h \in \mathbb{Z}^{0+}$ is equivalent to the attack stage $I_h \in \mathbb{Z}^{0+}$. Whenever the operator starts a new inspection at inspection stage $h \in \mathbb{Z}^{0+}$, RADAMS determines the AM action $a^h \in \mathcal{A}$ for the h -th inspection based on the stationary strategy $\sigma \in \Sigma : \mathcal{S} \mapsto \mathcal{A}$ that is adaptive to the category label of the h -th alert. We illustrate the timeline of the manual inspections and the AM strategies in green and blue, respectively, in Fig. 2. The solid and dashed green arrows indicate the inspected and uninspected alerts, respectively. The non-transparent and semi-transparent blue arrows indicate the emphasized and de-emphasized alerts, respectively. At inspection stage h , if $a^h = a_m$, RADAMS will make the next m alerts less noticeable; i.e., the alerts at attack stages $I_h + 1, \dots, I_h + m$ are de-emphasized. Denote $\bar{\kappa}_{SW}^{I_{h+1}-I_h, a^h}(s^{I_{h+1}} | s^{I_h})$ as the operator's switching probability to these de-emphasized alerts under the AM action $a^h \in \mathcal{A}$. Analogously to (1), the following holds for all $h \in \mathbb{Z}^{0+}$ and $a^h \in \mathcal{A}$, i.e.,

$$\sum_{I_{h+1}=I_h+1}^{\infty} \sum_{s^{I_{h+1}} \in \mathcal{S}} \bar{\kappa}_{SW}^{I_{h+1}-I_h, a^h}(s^{I_{h+1}} | s^{I_h}) \equiv 1, \forall s^{I_h} \in \mathcal{S}. \quad (3)$$

The deliberate de-emphasis on selective alerts brings the following tradeoff. On the one hand, these alerts do not increase the operator's stress level and the operator can pay sustained attention to the alert under inspection with high LOE and EIT. On the other hand, these alerts do not draw the operator's attention and the operator is less likely to switch to them during the real-time monitoring and inspections.

Since the operator may switch to inspect a de-emphasized alert with switching probability $\bar{\kappa}_{SW}^{I_{h+1}-I_h, a^h}$ (e.g., the h -inspection in Fig. 2), RADAMS recomputes the AM strategy and implements the new strategy whenever the operator has started to inspect a new alert. Although the operator can switch unpredictably, Proposition 1 shows that the transition of the inspected alerts' category labels is Markov.

Proposition 1. For a stationary AM strategy $\sigma \in \Sigma$, the set of random variables $(\mathbf{S}^{I_h}, \mathbf{T}^{I_h})_{h \in \mathbb{Z}^{0+}}$ is a Markov renewal process.

Proof. The sketch of the proof includes two steps. First, we prove that the state transition from s^{I_h} to $s^{I_{h+1}}$ is Markov for all $h \in \mathbb{Z}^{0+}$. Due to the uncertainty of switching in inspection, the transition stage \mathbf{I}_{h+1} is also a random variable for all $h \in \mathbb{Z}^{0+}$ and we can represent the transition probability as

$$\Pr(\mathbf{S}^{I_{h+1}} = s^{I_{h+1}} | s^{I_h}) = \sum_{l=1}^{\infty} \Pr(\mathbf{I}_{h+1} = I_h + l) \cdot \Pr(\mathbf{S}^{I_{h+1}} = s^{I_{h+1}} | s^{I_h}),$$

where $\Pr(\mathbf{I}_{h+1} = I_h + l)$ is the probability that the $(h+1)$ -th inspection happens at attack stage $I_h + l$. The term $\Pr(\mathbf{S}^{I_{h+1}} = s^{I_{h+1}} | s^{I_h})$ is Markov and can be computed based on κ_{CL} . The term $\Pr(\mathbf{I}_{h+1} = I_h + l)$ depends on $d(y_{EL}, s^{I_h+l}, \theta^{I_h+l}, \phi^{I_h+l})$, $\kappa_{SW}^{I_h}, \bar{\kappa}_{SW}^{I_h}, \tau^l$, for all $l' \in \{1, \dots, l\}$. Since $s^{I_h+l'}, \theta^{I_h+l'}, \phi^{I_h+l'}, l' \in \{1, \dots, l\}$, are all stochastically related to s^{I_h} and $s^{I_{h+1}}$ based on σ , κ_{AT} and κ_{CL} , the term $\Pr(\mathbf{I}_{h+1} = I_h + l)$ depends on s^{I_h} and $s^{I_{h+1}}$ for all $l \in \mathbb{Z}^+$.

Then, we show that the distribution of the inter-arrival time $\mathbf{T}_{IN}^{I_h, m} := \mathbf{T}^{I_{h+1}} - \mathbf{T}^{I_h}$ only depends on s^{I_h} and $s^{I_{h+1}}$. Analogously, the cumulative distribution function of $\mathbf{T}_{IN}^{I_h, m}$ is

$$\Pr(\mathbf{T}_{IN}^{I_h, m} \leq t) = \sum_{l=1}^{\infty} \Pr(\mathbf{I}_{h+1} = I_h + l) \cdot \Pr(\mathbf{T}_{IN}^{I_h, m} \leq t),$$

and hence we arrive at the Markov property. \square

B. Stage Cost and Expected Cumulative Cost

For each alert at attack stage $k \in \mathbb{Z}^{0+}$, RADAMS assigns a stage cost $\bar{c}(w^k, s^k)$ based on the alert response $w^k \in \mathcal{W}$ and the category label $s^k \in \mathcal{S}$. The value of the cost can be estimated by the salary of SOC analysts and the estimated loss of the associated attack. For example, $\bar{c}(w_{UN}, s^{I_h})$ and $\bar{c}(w_{NI}, s^{I_h})$ are positive costs as those alerts without a complete response incur additional workloads. The delayed inspections also expose the organization to the threats of time-sensitive attacks. On the other hand, $\bar{c}(w_{FE}, s^{I_h})$ and $\bar{c}(w_{RE}, s^{I_h})$ are negative costs as the alerts with complete alert response w_{FE} and w_{RE} reduce the workload of tier 2 SOC analysts and enable them to obtain threat intelligence.

When the operator starts a new inspection at inspection stage $h+1$, RADAMS will evaluate the effectiveness of the AM strategy for the h -th inspection. The performance evaluation is reflected by the Expected Consolidated Cost

(ECoC) $c : \mathcal{S} \times \mathcal{A} \mapsto \mathbb{R}$ at each inspection stage $h \in \mathbb{Z}^{0+}$. We denote the realization of $c(s^h, a^h)$ as the Consolidated Cost (CoC) $\tilde{c}^h(s^h, a^h)$. Since the AM strategy σ at each inspection stage can affect the future human inspection process and the alert responses, we define the Expected Cumulative Cost (ECuC) $u(s^h, \sigma) := \sum_{h=0}^{\infty} \gamma^h c(s^h, \sigma(s^h))$ under adaptive strategy $\sigma \in \Sigma$ as the long-term performance measure. The goal of the assistive technology is to design the optimal adaptive strategy $\sigma^* \in \Sigma$ that minimizes the ECuC u under the presented IDoS attack based on the category label $s^h \in \mathcal{S}$ at each inspection stage h . We define $v^*(s^h) := \min_{\sigma \in \Sigma} u(s^h, \sigma)$ as the optimal ECuC when the category label is $s^h \in \mathcal{S}$. We refer to the *default AM strategy* $\sigma^0 \in \Sigma$ as the one when no AM action is applied under all category labels, i.e., $\sigma^0(s^h) = a_0, \forall s^h \in \mathcal{S}$.

C. Reinforcement Learning

Due to the absence of the following exact model parameters, RADAMS has to learn the optimal AM strategy $\sigma^* \in \Sigma$ based on the operator's alert responses in real time.

- Parameters of the IDoS attack model (e.g., κ_{AT} and z) and the alert generation model (e.g., o) in Section III.
- Parameters of the human attention model (e.g., f_{LOE} and f_{SI}), inspection model (e.g., $\kappa_{SW}^{\Delta k}$, $\bar{\kappa}_{SW}^{I_{h+1}-I_h, a^h}$, and d), and alert response model (e.g., y_{EL} and p_{SP}) in Section IV.

Define $Q^h(s^h, a^h)$ as the estimated ECuC during the h -th inspection when the category label is $s^h \in \mathcal{S}$ and the AM action is a^h . Based on Proposition 1, the state transition is Markov, which enables Q-learning as follows.

$$Q^{h+1}(s^h, a^h) := (1 - \alpha^h(s^h, a^h))Q^h(s^h, a^h) + \alpha^h(s^h, a^h)[\tilde{c}^h(s^h, a^h) + \gamma \min_{a' \in \mathcal{A}} Q^h(s^{h+1}, a')], \quad (4)$$

where s^h and s^{h+1} are the observed category labels of the alerts at the attack stage I_h and I_{h+1} , respectively. When the learning rate $\alpha^h(s^h, a^h) \in (0, 1)$ satisfies $\sum_{h=0}^{\infty} \alpha^h(s^h, a^h) = \infty, \sum_{h=0}^{\infty} (\alpha^h(s^h, a^h))^2 < \infty, \forall s^h \in \mathcal{S}, \forall a^h \in \mathcal{A}$, and all state-action pairs are explored infinitely, $\min_{a' \in \mathcal{A}} Q^h(s^h, a')$ converges to the optimal ECuC $v^*(s^h)$ with probability 1 as $h \rightarrow \infty$. At each inspection stage $h \in \mathbb{Z}^{0+}$, RADAMS selects AM strategy $a^h \in \mathcal{A}$ based on the ϵ -greedy policy; i.e., RADAMS chooses a random action with a small probability $\epsilon \in [0, 1]$, and the optimal action $\arg \min_{a' \in \mathcal{A}} Q^h(s^h, a')$ with probability $1 - \epsilon$.

We present the algorithm to learn the adaptive AM strategy based on the operator's real-time alert monitoring and inspection process in Algorithm 1. Each simulation run corresponds to the operator's work shift of 24 hours at the SOC. Since the SOC can receive over 10 thousand of alerts in each work shift, we can use infinite horizon to approximate the total number of attack stages $K > 10,000$. Whenever the operator starts to inspect a new alert at inspection stage I_{h+1} , RADAMS applies Q-learning in (4) based on the category label s^{h+1} of the newly arrived alert and determines the AM action a^{h+1} for the $h+1$ inspection based on the ϵ -greedy policy as shown in lines 12 and 19 of Algorithm 1. The CoC $\tilde{c}^h(s^h, a^h)$ of the h -th inspection under the AM action $a^h \in \mathcal{A}$ and the category label

Algorithm 1: Algorithm to Learn the Adaptive AM strategy based on the Operator's Real-Time Alert Inspection

```

1 Input  $K$ : The total number of attack stages;
2 Initialize The operator starts the  $h$ -th inspection under
   AM action  $a^h \in \mathcal{A}$ ;  $I_h = k_0$ ;  $\tilde{c}^h(s^h, a^h) = 0$ ;
3 for  $k \leftarrow k_0 + 1$  to  $K$  do
4   if The operator has finished the  $I_h$ -th alert (i.e.,
    $EIT > AITN$ ), then
5     if Capable (i.e.,  $rand \leq p_{SP}(y_{EL}, s^k, \theta^k, \phi^k)$ ) then
6       Dismiss (i.e.,  $w^{I_h} = w_{FE}$ ) or escalate (i.e.,
        $w^{I_h} = w_{RE}$ ) the  $I_h$ -th alert;
7     else
8       Queue up the  $I_h$ -th alert, i.e.,  $w^{I_h} = w_{UN}$ ;
9     end
10     $\tilde{c}^h(s^h, a^h) = \tilde{c}^h(s^h, a^h) + \bar{c}(w^{I_h}, s^h)$ ;
11     $I_{h+1} \leftarrow k$ ; The operator starts to inspect the  $k$ -th
       alert with category label  $s^{h+1}$ ;
12    Update  $Q^{h+1}(s^h, a^h)$  via (4) and obtain the AM
       action  $a^{h+1}$  by  $\epsilon$ -greedy policy;
13     $\tilde{c}^{h+1}(s^{h+1}, a^{h+1}) = 0$ ;  $h \leftarrow h + 1$ ;
14  else
15    if The operator chooses to switch or The MAD is
       reached, i.e.,  $t^k - t^{I_h} \geq D_{max}$  then
16      Queue up the  $I_h$ -th alert (i.e.,  $w^{I_h} = w_{UN}$ );
17       $\tilde{c}^h(s^h, a^h) = \tilde{c}^h(s^h, a^h) + \bar{c}(w_{UN}, s^h)$ ;
18       $I_{h+1} \leftarrow k$ ; The operator starts to inspect the  $k$ -th
       alert with category label  $s^{h+1}$ ;
19      Update  $Q^{h+1}(s^h, a^h)$  via (4) and obtain the AM
       action  $a^{h+1}$  by  $\epsilon$ -greedy policy;
20       $\tilde{c}^{h+1}(s^{h+1}, a^{h+1}) = 0$ ;  $h \leftarrow h + 1$ ;
21    else
22      The operator continues the inspection of the
        $I_h$ -th alert with decreased LOE;
23      The  $k$ -th alert is queued up for delayed
       inspection (i.e.,  $w^k = w_{NI}$ );
24       $\tilde{c}^h(s^h, a^h) = \tilde{c}^h(s^h, a^h) + \bar{c}(w_{NI}, s^h)$ ;
25    end
26  end
27 end
28 Return  $Q^h(s, a), \forall s \in \mathcal{S}, a \in \mathcal{A}$ ;

```

s^h of the inspected alert can be computed iteratively based on the stage cost $\bar{c}(w^k, s^k)$ of the alerts during the attack stage $k \in \{I_h, \dots, I_{h+1} - 1\}$ as shown in lines 13, 20, and 24 of Algorithm 1.

VI. THEORETICAL ANALYSIS

In Section VI, we focus on the class of ambitious operators who attempt to inspect all alerts, i.e., $\kappa_{SW}(s^{k+\Delta k} | s^k) = \mathbf{1}_{\{\Delta k=1\}}, \forall s^k, s^{k+\Delta k} \in \mathcal{S}, \forall \Delta k \in \mathbb{Z}^+$. To assist this class of operators, the implemented AM action $a_m, m \in \{0, 1, \dots, M\}$, chooses to make the selected alerts fully unnoticeable. Then, under $a_m \in \mathcal{A}$, the operator at inspection stage h can pay sustained attention to inspect the alert of category label $s^h \in \mathcal{S}$ for $m+1$ attack stages. Moreover,

the operator switches to the new alert at attack stage I_{h+1} , i.e., $\sum_{s^{I_h+m+1} \in \mathcal{S}} \tilde{K}_{SW}^{I_{h+1}-I_h, a_m}(s^{I_h+m+1} | s^{I_h}) = \mathbf{1}_{\{I_{h+1}-I_h=m+1\}}$. Throughout the section, we omit the variable of the expertise level y_{EL} in functions d, \bar{d}, p_{SP} , and p_{CG} as y_{EL} is a constant for all attack stages.

A. Security Metrics

We propose two security metrics in Definition 3 to evaluate the performance of ambitious operators under IDoS attacks and different AM strategies. The first metric, denoted as $p_{UN}(s^{I_h}, a^h)$, is the probability that the operator chooses w_{UN} during the h -th inspection under the category label $s^{I_h} \in \mathcal{S}$ and AM action $a^h \in \mathcal{A}$. This metric reflects the Attentional Deficiency Level (ADL) of the IDoS attack. For example, as the attackers generate more feints at a higher frequency, the operator is persistently distracted by the new alerts, and it becomes unlikely for him to fully respond to an alert. The ADL $p_{UN}(s^{I_h}, a^h)$ is high in this scenario. We use the ECuC $u(s^{I_h}, \sigma)$ as the second metric that evaluates the *IDoS risk* under the category label $s^{I_h} \in \mathcal{S}$ and the AM strategy $\sigma \in \Sigma$. For both metrics, smaller values are preferred.

Definition 3 (Attentional Deficiency Level and Risk). Under category label $s^{I_h} \in \mathcal{S}$ and the stationary AM strategy $\sigma \in \Sigma$, we define $p_{UN}(s^{I_h}, \sigma(s^{I_h}))$ and $u(s^{I_h}, \sigma)$ as the Attentional Deficiency Level (ADL) and the risk of the IDoS attacks defined in Section III, respectively.

B. Closed-Form Computations

The Markov renewal process that characterizes the IDoS attack or the associated alert sequence follows a Poisson process when Condition 1 holds.

Condition 1 (Poisson Arrival). The inter-arrival time τ^k for all attack stage $k \in \mathbb{Z}^{0+}$ is exponentially distributed with the same arrival rate denoted by $\beta > 0$, i.e., $z(\tau | \theta^{k+1}, \phi^{k+1}, \theta^k, \phi^k) = \beta e^{-\beta \tau}, \tau \in [0, \infty)$ for all $\theta^{k+1}, \theta^k \in \Theta$ and $\phi^{k+1}, \phi^k \in \Phi$.

Recall that random variable $T_{IN}^{I_h, m}$ represents the inspection time of the I_h -th alert under the AM action $a^h = a_m \in \mathcal{A}$. For the ambitious operators under AM action $a_m \in \mathcal{A}$ at inspection stage h , the next inspection happens at attack stage $I_{h+1} = I_h + m + 1$. Thus, I_{h+1} is no longer a random variable. As a summation of $m + 1$ i.i.d. exponential distributed random variables of rate β , $T_{IN}^{I_h, m}$ follows an *Erlang distribution* denoted by \bar{z} with shape $m + 1$ and rate $\beta > 0$ when condition 1 holds, i.e., $\bar{z}(\tau) = \frac{\beta^{m+1} \tau^m e^{-\beta \tau}}{m!}, \tau \in [0, \infty)$.

Denote $p_{SD}^h(w^{I_h} | s^{I_h}, a^h; \theta^{I_h}, \phi^{I_h})$ as the probability that the operator makes alert response w^{I_h} at inspection stage h . To obtain a theoretical underpinning, we consider the case where the AITN equals the average inspection time, i.e., $d(s^k, \theta^k, \phi^k) = \bar{d}(s^k, \theta^k, \phi^k)$. Then, the operator under AM action a_m makes a complete alert response (i.e., $w^{I_h} \in \{w_{FE}, w_{RE}\}$) at inspection stage h for category label s^{I_h} if the inspection time $T_{IN}^{I_h, m}$ is greater than the AITN. The probability of the above event can be represented

$$\text{as } \int_{d(s^{I_h}, \theta^{I_h}, \phi^{I_h})}^{\infty} p_{SP}(s^{I_h}, \theta^{I_h}, \phi^{I_h}) \bar{z}(\tau) d\tau = p_{SP}(s^{I_h}, \theta^{I_h}, \phi^{I_h}) \cdot \sum_{n=0}^m \frac{1}{n!} e^{-\beta d(s^{I_h}, \theta^{I_h}, \phi^{I_h})} (\beta d(s^{I_h}, \theta^{I_h}, \phi^{I_h}))^n, \text{ which leads to}$$

$$p_{SD}^h(w_{UN} | s^{I_h}, a_m; \theta^{I_h}, \phi^{I_h}) = 1 - p_{SP}(s^{I_h}, \theta^{I_h}, \phi^{I_h}) \cdot \sum_{n=0}^m \frac{1}{n!} e^{-\beta d(s^{I_h}, \theta^{I_h}, \phi^{I_h})} (\beta d(s^{I_h}, \theta^{I_h}, \phi^{I_h}))^n. \quad (5)$$

Then, the ADL $p_{UN}(s^{I_h}, a^h)$ can be computed as

$$\sum_{\theta^{I_h} \in \Theta, \phi^{I_h} \in \Phi} \Pr(\theta^{I_h}, \phi^{I_h} | s^{I_h}) \cdot p_{SD}^h(w_{UN} | s^{I_h}, a^h; \theta^{I_h}, \phi^{I_h}), \quad (6)$$

where the conditional probability $\Pr(\theta^{I_h}, \phi^{I_h} | s^{I_h})$ can be computed via the Bayesian rule, i.e., $\Pr(\theta^{I_h}, \phi^{I_h} | s^{I_h}) = \frac{o(s^{I_h} | \theta^{I_h}, \phi^{I_h}) b(\theta^{I_h}, \phi^{I_h})}{\sum_{\theta^{I_h} \in \Theta, \phi^{I_h} \in \Phi} o(s^{I_h} | \theta^{I_h}, \phi^{I_h}) b(\theta^{I_h}, \phi^{I_h})}$.

We can compute the ECoC $c(s^{I_h}, a_m)$ explicitly as

$$c(s^{I_h}, a_m) = m \bar{c}(w_{NI}, s^{I_h}) + \sum_{\theta^{I_h} \in \Theta, \phi^{I_h} \in \Phi} \Pr(\theta^{I_h}, \phi^{I_h} | s^{I_h}) \cdot \sum_{w^{I_h} \in \mathcal{W}} p_{SD}^h(w^{I_h} | s^{I_h}, a_m; \theta^{I_h}, \phi^{I_h}) \bar{c}(w^{I_h}, s^{I_h}). \quad (7)$$

For prudent operators in Section IV-A, we have

$$p_{SD}^h(w_i | s^{I_h}, a^h; \theta_i, \phi^{I_h}) = 1 - p_{SD}^h(w_{UN} | s^{I_h}, a^h; \theta_i, \phi^{I_h}), \quad (8)$$

for all $i \in \{FE, RE\}, s^{I_h} \in \mathcal{S}, a^h \in \mathcal{A}, \phi^{I_h} \in \Phi, h \in \mathbb{Z}^{0+}$. Plugging (8) into (7), we can simplify the ECoC $c(s^{I_h}, a_m)$ as

$$c(s^{I_h}, a_m) = \sum_{\phi^{I_h} \in \Phi} \sum_{i \in \{FE, RE\}} \Pr(\theta_i, \phi^{I_h} | s^{I_h}) \cdot p_{SD}^h(w_i | s^{I_h}, a_m; \theta_i, \phi^{I_h}) \cdot [\bar{c}(w_i, s^{I_h}) - \bar{c}(w_{UN}, s^{I_h})] + m \bar{c}(w_{NI}, s^{I_h}) + \bar{c}(w_{UN}, s^{I_h}). \quad (9)$$

As shown in Proposition 2, the ADL and the risk are monotone function of $\beta d(s^{I_h}, \theta^{I_h}, \phi^{I_h})$ for each AM strategy.

Proposition 2. If condition 1 holds, then the ADL $p_{UN}(s^{I_h}, \sigma(s^{I_h}))$ and the risk $u(s^{I_h}, \sigma)$ of an IDoS attack under category label $s^{I_h} \in \mathcal{S}$ and AM strategy $\sigma \in \Sigma$ increase in the value of the product $\beta d(s^{I_h}, \theta^{I_h}, \phi^{I_h})$.

Proof. First, since $p_{SD}^h(w_{UN})$ in (5) increases monotonously with respect to the product $\beta d(s^{I_h}, \theta^{I_h}, \phi^{I_h})$, the values of $p_{SD}^h(w_{FE})$ and $p_{SD}^h(w_{RE})$ in (8) decrease monotonously with respect to the product. Plugging (5) into (6), we obtain that $p_{UN}(s^{I_h}, a_m)$ in (10) under any $a_m \in \mathcal{A}$ and $s^{I_h} \in \mathcal{S}$ is a summation of functions increasing in $\beta d(s^{I_h}, \theta^{I_h}, \phi^{I_h})$.

$$p_{UN}(s^{I_h}, a_m) = \sum_{\phi^{I_h} \in \Phi} \sum_{i \in \{FE, RE\}} \Pr(\theta_i, \phi^{I_h} | s^{I_h}) [1 - p_{SD}^h(w_i | s^{I_h}, a^h; \theta_i, \phi^{I_h})] \cdot \sum_{n=0}^m \frac{1}{n!} e^{-\beta d(s^{I_h}, \theta_i, \phi^{I_h})} (\beta d(s^{I_h}, \theta_i, \phi^{I_h}))^n. \quad (10)$$

Second, since $\bar{c}(w_{FE}, s^{I_h})$ and $\bar{c}(w_{RE}, s^{I_h})$ are negative and $\bar{c}(w_{UN}, s^{I_h})$ is positive, the ECoC in (9) decreases with $\beta d(s^{I_h}, \theta^{I_h}, \phi^{I_h})$ under any $a_m \in \mathcal{A}$ and $s^{I_h} \in \mathcal{S}$. Then, the risk also decreases with the product due to the monotonicity of the Bellman operator [34]. \square

Remark 1 (Product Principle of Attention (PPoA)). On the one hand, as β increases, the feint and real attacks arrive at a higher frequency on average, resulting in a higher demand of attention resources from the human operator. On the other

hand, as $d(s^{I_h}, \theta^{I_h}, \phi^{I_h})$ increases, the human operator requires a longer inspection time to determine the attack's type, leading to a lower supply of attention resources. Proposition 2 characterizes the PPoA that the ADL and the risk of IDoS attacks depend on the product of the supply and demand of attention resources for any stationary AM strategy $\sigma \in \Sigma$.

C. Fundamental Limits under AM strategies

Section VI-C aims to show the fundamental limits of the IDoS attack's ADL, the ECoC, and the risk under different AM strategies. Define the shorthand notation: $\underline{p}(s^{I_h}) := \sum_{\phi^{I_h} \in \Phi} \sum_{i \in \{FE, RE\}} \Pr(\theta_i, \phi^{I_h} | s^{I_h}) p_{CG}(s^{I_h}, \theta_i, \phi^{I_h})$.

Lemma 1. *If Condition 1 holds and $M \rightarrow \infty$, then for each $s^{I_h} \in \mathcal{S}$, the ADL $p_{UN}(s^{I_h}, a_m)$ decreases strictly to $\underline{p}(s^{I_h})$ as m increases.*

Proof. Since $\frac{1}{n!} e^{-\beta d(s^{I_h}, \theta^{I_h}, \phi^{I_h})} (\beta d(s^{I_h}, \theta^{I_h}, \phi^{I_h}))^n > 0$ for all $m \in \{0, \dots, M\}$, the value of $p_{UN}(s^{I_h}, a_m)$ in (10) strictly decreases as m increases. Moreover, since $\lim_{m \rightarrow \infty} \sum_{n=0}^m \frac{1}{n!} e^{-\beta d(s^{I_h}, \theta^{I_h}, \phi^{I_h})} (\beta d(s^{I_h}, \theta^{I_h}, \phi^{I_h}))^n = 1$, we have $\min_{m \in \{0, \dots, M\}} p_{UN}(s^{I_h}, a_m) = \underline{p}(s^{I_h})$ for all $s^{I_h} \in \mathcal{S}$. \square

Remark 2 (Fundamental Limit of ADL). *Lemma 1 characterizes that the minimum ADL under all AM strategies $a_m \in \mathcal{A}$ is $\underline{p}(s^{I_h})$. The value of $\underline{p}(s^{I_h})$ depends on both the operator's capacity gap $p_{CG}(s^{I_h}, \theta_{FE}, \phi^{I_h})$ and the frequency of feint and real attacks with different targets, i.e., $\Pr(\theta^{I_h}, \phi^{I_h} | s^{I_h}), \forall \theta^{I_h} \in \Theta, \phi^{I_h} \in \Phi$.*

Denote the expected reward of making a complete alert response (i.e., the rewards to dismiss feints and escalate real attacks) as

$$\begin{aligned} \lambda(s^{I_h}, m, \phi^{I_h}) &= \sum_{i \in \{FE, RE\}} \bar{c}(w_i, s^{I_h}) \cdot \Pr(\theta_i, \phi^{I_h} | s^{I_h}) \\ &\cdot p_{SP}^h(s^{I_h}, \theta_i, \phi^{I_h}) \cdot \left[\sum_{n=0}^m \frac{1}{n!} e^{-\beta d(s^{I_h}, \theta_i, \phi^{I_h})} (\beta d(s^{I_h}, \theta_i, \phi^{I_h}))^n \right]. \end{aligned}$$

Combining (10) and (9), we can rewrite ECoC as a combination of the following three terms in (11).

$$\begin{aligned} c(s^{I_h}, a_m) &= p_{UN}(s^{I_h}, a_m) \bar{c}(w_{UN}, s^{I_h}) \\ &+ m \bar{c}(w_{NI}, s^{I_h}) + \sum_{\phi^{I_h} \in \Phi} \lambda(s^{I_h}, m, \phi^{I_h}). \end{aligned} \quad (11)$$

Based on Lemma 1, the first term $p_{UN}(s^{I_h}, a_m) \bar{c}(w_{UN}, s^{I_h})$ and the third term $\sum_{\phi^{I_h} \in \Phi} \lambda(s^{I_h}, m, \phi^{I_h})$ decrease in m while the second term $m \bar{c}(w_{NI}, s^{I_h})$ in (11) increases in m linearly at the rate of $\bar{c}(w_{NI}, s^{I_h})$. The tradeoff among the three terms is summarized below.

Remark 3 (Tradeoff among ADL, Reward of Alert Attention, and Impact for Alert Inattention). *Based on Lemma 1 and (11), increasing m reduces the ADL, and achieves a higher reward of completing the alert response. However, the increase of m also linearly increases the impact for alert inattention represented by $m \bar{c}(w_{NI}, s^{I_h})$, the cost of uninspected alerts. Thus, we need to strike a balance among these terms to reduce the IDoS risk.*

Define $\lambda_{min}(s^{I_h}, \phi^{I_h}) := \sum_{i \in \{FE, RE\}} \bar{c}(w_i, s^{I_h}) \Pr(\theta_i, \phi^{I_h} | s^{I_h}) p_{SP}^h(s^{I_h}, \theta_i, \phi^{I_h})$, $\lambda_{max}^{\varepsilon_0}(s^{I_h}, \phi^{I_h}) := (1 - \varepsilon_0) \lambda_{min}(s^{I_h}, \phi^{I_h})$, $c_{min}(s^{I_h}) := \sum_{\phi^{I_h} \in \Phi} \lambda_{min}(s^{I_h}, \phi^{I_h}) + \underline{p}(s^{I_h}) \bar{c}(w_{UN}, s^{I_h}) + m \bar{c}(w_{NI}, s^{I_h})$, and $c_{max}^{\varepsilon_0}(s^{I_h}) := \sum_{\phi^{I_h} \in \Phi} \lambda_{max}^{\varepsilon_0}(s^{I_h}, \phi^{I_h}) + [\underline{p}(s^{I_h}) + \varepsilon_0 (1 - \underline{p}(s^{I_h}))] \bar{c}(w_{UN}, s^{I_h}) + m \bar{c}(w_{NI}, s^{I_h})$.

Proposition 3. *Consider the scenario where Condition 1 holds and $M > \underline{m}(s^{I_h})$. For any $\varepsilon_0 \in (0, 1]$ and $s^{I_h} \in \mathcal{S}$, there exists $\underline{m}(s^{I_h}) \in \mathbb{Z}^+$ such that $c(s^{I_h}, a_m) \in [c_{min}(s^{I_h}), c_{max}^{\varepsilon_0}(s^{I_h})], \forall a_m \in \mathcal{A}$, when $m \geq \underline{m}(s^{I_h})$. Moreover, the lower bound $c_{min}(s^{I_h})$ and the upper bound $c_{max}^{\varepsilon_0}(s^{I_h})$ increase in m linearly at the same rate $\bar{c}(w_{NI}, s^{I_h})$.*

Proof. For any $\varepsilon_0 \in (0, 1]$, there exists $\underline{m}(s^{I_h}) \in \mathbb{Z}^+$ such that $\sum_{n=0}^m \frac{1}{n!} e^{-\beta d(s^{I_h}, \theta^{I_h}, \phi^{I_h})} (\beta d(s^{I_h}, \theta^{I_h}, \phi^{I_h}))^n \in [1 - \varepsilon_0, 1]$ when $m \geq \underline{m}(s^{I_h})$. Based on Lemma 1, if $m > \underline{m}(s^{I_h})$, then $p_{UN}(s^{I_h}, a_m) \in [\underline{p}(s^{I_h}), \underline{p}(s^{I_h}) + \varepsilon_0 (1 - \underline{p}(s^{I_h}))]$. Plugging it into (11), we obtain the results. \square

Let $\sigma^m \in \Sigma$ denote the AM strategy that chooses to de-emphasize the next $m \geq \underline{m}(s^{I_h})$ alerts for all category label $s^{I_h} \in \mathcal{S}$. The monotonicity of the Bellman operator [34] leads to the following corollary.

Corollary 1. *Consider the scenario where Condition 1 holds and $M > \underline{m}(s^{I_h})$. For any $\varepsilon_0 \in (0, 1]$ and $s^{I_h} \in \mathcal{S}$, the upper and lower bounds of the risk $u(s^{I_h}, \sigma^m)$ increase in m linearly at the same rate of $\bar{c}(w_{NI}, s^{I_h})$.*

Remark 4 (Fundamental Limit of ECoC and Risk). *Proposition 3 and Corollary 1 show that the maximum length of the de-emphasized alerts for any $s^{I_h} \in \mathcal{S}$ should not exceed $\underline{m}(s^{I_h})$ to reduce the ECoC and the risk of IDoS attacks.*

VII. CASE STUDY

The following section presents case studies to demonstrate the impact of IDoS attacks on human operators' alert inspections and alert responses, and further illustrate the effectiveness of RADAMS. Throughout the section, we adopt the attention model in Section IV.

A. Experiment Setup

We consider an IDoS attack targeting either the Programmable Logic Controllers (PLCs) in the physical layer or the data centers in the cyber layer of an ICS. We denote these two targets as ϕ_P and ϕ_C , respectively. They constitute the binary set of attack targets $\Phi = \{\phi_P, \phi_C\}$ defined in Section III-A. The SOC of the ICS is in charge of monitoring, inspecting, and responding to both the cyber and the physical alerts. We consider two system-level metrics defined in Section III-B, the source $\mathcal{S}_{SO} = \{s_{SO,P}, s_{SO,C}\}$ and the criticality $\mathcal{S}_{CR} = \{s_{CR,L}, s_{CR,H}\}$, i.e., $\mathcal{S} = \mathcal{S}_{SO} \times \mathcal{S}_{CR}$. Let $s_{SO,P}$ and $s_{SO,C}$ represent the source of physical and cyber layers, respectively. We assume that the alert triage process can accurately identify the source of attacks, i.e., $\Pr(s_{SO,i} | \phi_j) = \mathbf{1}_{\{i=j\}}$, $\forall i, j \in \{P, C\}$. Let $s_{CR,L}$ and $s_{CR,H}$ represent low and high criticality, respectively. We assume that the triage process cannot accurately identify feints as low criticality and real attacks as high criticality. The revelation kernel is separable and takes the form

of $o(s_{SO}, s_{CR} | \theta_i, \phi_j) = \Pr(s_{SO} | \phi_j) \cdot \Pr(s_{CR} | \theta_i), s_{SO} \in \mathcal{S}_{SO}, s_{CR} \in \mathcal{S}_{CR}, i \in \{FE, RE\}, j \in \{P, C\}$. We choose the values of o so that the attack is more likely to be feint (resp. real) when the criticality level is low (resp. high).

The inter-arrival time at attack stage $k \in \mathbb{Z}^{0+}$ follows an exponential distribution with rate $\beta(\theta^k, \theta^{k+1})$ parameterized by the attack's type θ^k, θ^{k+1} . Thus, the average inter-arrival time $\mu(\theta^k, \theta^{k+1}) := 1/\beta(\theta^k, \theta^{k+1})$ also depends on the attack's type at the current and the next attack stages as shown in Table I. We choose the benchmark values based on the literature (e.g., [18], [35] and the references within) and attacks can change these values in different IDoS attacks.

TABLE I: Benchmark values of the average inter-arrival time $\mu(\theta^k, \theta^{k+1}) = 1/\beta(\theta^k, \theta^{k+1}), \forall \theta^k, \theta^{k+1} \in \Theta$.

Average inter-arrival time from feints to real attacks	6s
Average inter-arrival time from real attacks to feints	10s
Average inter-arrival time between feints	15s
Average inter-arrival time between real attacks	8s

The average inspection time \bar{d} in Section IV-C depends on the criticality s_{CR}^k and attack's type θ^k at attack stage $k \in \mathbb{Z}^{0+}$ as shown in Table II. We choose the benchmark values of $\bar{d}(s_{CR}^k, \theta^k)$ based on [18], and these values can change for different human operators and IDoS attacks. We add a random noise uniformly distributed in $[-5, 5]$ to the average inspection time to simulate the AITN.

TABLE II: Benchmark values of the average inspection time $\bar{d}(s_{CR}^k, \theta^k), \forall \theta^k \in \Theta, s_{CR}^k \in \mathcal{S}_{CR}$.

Average time to inspect feints of low criticality	6s
Average time to inspect feints of high criticality	8s
Average time to inspect real attacks of low criticality	15s
Average time to inspect real attacks of high criticality	20s

The stage cost $\bar{c}(w^k, s_{SO}^k)$ at attack stage $k \in \mathbb{Z}^{0+}$ in Section V-B depends on the alert response $w^k \in \mathcal{W}$ and the source $s_{SO}^k \in \mathcal{S}_{SO}$. We determine the benchmark values of $\bar{c}(w^k, s_{SO}^k)$ per alert in Table III based on the salary of the SOC analysts and the estimated loss of the associated attacks.

TABLE III: The benchmark values of the stage cost $\bar{c}(w^k, s_{SO}^k), \forall w^k \in \mathcal{W}, s_{SO}^k \in \mathcal{S}_{SO}$.

Reward of dismissing feints w_{FE}	\$80
Reward of identifying real attacks w_{RE} in physical layer	\$500
Reward of identifying real attacks w_{RE} in cyber layer	\$100
Cost of incomplete alert response w_{UN} or w_{NI}	\$300

B. Analysis of Numerical Results

We plot the dynamics of the operator's alert responses in Fig. 3 under the benchmark experiment setup in Section VII-A. We use green, purple, orange, and yellow to represent w_{UN} , w_{NI} , w_{FE} , and w_{RE} , respectively. The heights of squares are also used to distinguish the four categories.

1) *Adaptive Learning during the Real-Time Monitoring and Inspection:* Based on Algorithm 1, we illustrate the learning process of the estimated ECUC $Q^h(s^{I_h}, a^h)$ for all $s^{I_h} \in \mathcal{S}$ and $a^h \in \mathcal{A}$ at each inspection stage $h \in \mathbb{Z}^{0+}$ in Fig. 4. We choose $\alpha^h(s^{I_h}, a^h) = \frac{k_c}{k_{TI}(s^{I_h}) - 1 + k_c}$ as the learning rate where $k_c \in (0, \infty)$

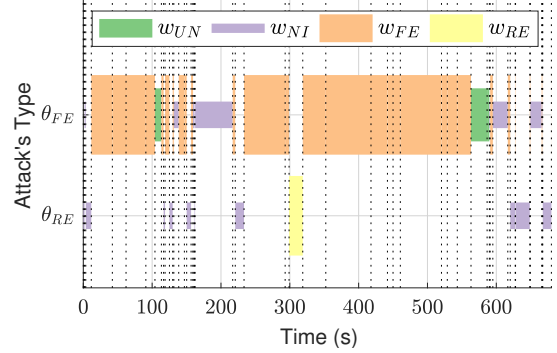


Fig. 3: Alert response $w^k \in \mathcal{W}$ for the k -th attack whose type is shown in the y -axis. The k -th vertical dash line represents the k -th alert's arrival time t^k .

is a constant parameter and $k_{TI}(s^{I_h}) \in \mathbb{Z}^{0+}$ is the number of visits to $s^{I_h} \in \mathcal{S}$ up to stage $h \in \mathbb{Z}^{0+}$. Here, the AM action a^h is implemented randomly at each inspection stage h , i.e., $\varepsilon = 1$. Thus, all four AM actions ($M = 3$) are explored equally on average for each $s^{I_h} \in \mathcal{S}$ as shown in Fig. 4. Since the number of visits to different category labels depends on the transition probability κ_{AT} , the learning stages for four category labels are of different lengths.

We denote category labels $(s_{SO,P}, s_{CR,L})$, $(s_{SO,P}, s_{CR,H})$, $(s_{SO,C}, s_{CR,L})$, and $(s_{SO,C}, s_{CR,H})$ in blue, red, green, and black, respectively. To distinguish four AM actions, a deeper color represents a larger $m \in \{0, 1, 2, 3\}$ for each category label $s_{SO,i}, s_{CR,j}, i \in \{P, C\}, j \in \{H, L\}$. The inset black box magnifies the selected area. The optimal strategy $\sigma^* \in \Sigma$ is to take a_3 for all category labels. The risk $v^*(s^{I_h}) = u(s^{I_h}, \sigma^*)$ under the optimal strategy has the approximated values of \$1153, \$1221, \$1154, and \$1358 for the above category labels in blue, red, green, and black, respectively. We also simulate the operator's real-time monitoring and inspection under IDoS attacks when AM strategy is not applied based on Algorithm 1. The risks $v^0(s^{I_h}) := u(s^{I_h}, \sigma^0)$ under the default AM strategy $\sigma^0 \in \Sigma$ have the approximated values of \$1377, \$1527, \$1378, and \$1620 for the category label $(s_{SO,P}, s_{CR,L})$, $(s_{SO,P}, s_{CR,H})$, $(s_{SO,C}, s_{CR,L})$, and $(s_{SO,C}, s_{CR,H})$, respectively. These results illustrate that the optimal AM strategy $\sigma^* \in \Sigma$ can significantly reduce the risk under IDoS attacks for all category labels and the reduction percentage can be as high as 20%.

We further investigate the IDoS risk under the optimal AM strategy σ^* as follows. As illustrated in Fig. 4, when the criticality level is high (i.e., the attack is more likely to be real), the attacks targeting cyber layers (denoted in black) result in a higher risk than the one targeting physical layers (denoted in red). This asymmetry results from the different rewards of identifying real attacks in physical or cyber layers denoted in Table III. Since dismissing feints bring the same reward in physical and cyber layers, the attacks targeting physical or cyber layers result in similar IDoS risks when the criticality level is low. Within physical or cyber layers, high-criticality alerts result in a higher risk than low-criticality alerts do.

The value of $Q^h(s^{I_h}, a_m), m \in \{0, 1, 2\}$, represents the risk when RADAMS deviates to sub-optimal AM action a_m for

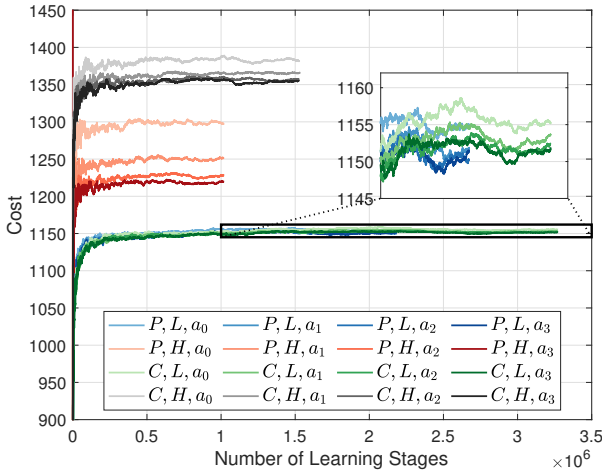


Fig. 4: The convergence of the estimated ECU-C $Q^h(s^h, a^h)$ vs. the number of inspection stages.

a single category label $s^h \in \mathcal{S}$. As illustrated by the red and black lines in Fig. 4, this single deviation can increase the risk under alerts of high criticality. However, it hardly increases the risk under alerts of low criticality as illustrated by the green and blue lines in the inset black box of Fig. 4. These results illustrate that we can deviate from the optimal AM strategy to sub-optimal ones for some category labels with approximately equivalent risk, which we refer to as the *attentional risk equivalency* in Remark 5.

Remark 5 (Attentional Risk Equivalency). *The above results illustrate that we can contain the IDoS risk by selecting proper sub-optimal strategies. If applying the optimal AM strategy σ^* is costly, then RADAMS can choose not to apply AM strategy for $(s_{SO,C}, s_{CR,L})$ or $(s_{SO,P}, s_{CR,L})$ without significantly increasing the IDoS risks.*

2) *Optimal AM Strategy and Resilience Margin under Different Stage Costs:* We define *resilience margin* as the difference of the risks under the optimal and the default AM strategies. We investigate how the cost of incomplete alert response in Table III affects the optimal AM strategy and the resilience margin in Fig. 5.

As shown in the upper figure, the optimal strategy remains to choose AM action a_3 when the alert is of high criticality. When the alert is of low criticality, then as the cost increases, the optimal AM strategy changes sequentially from a_3, a_2 , and a_1 to a_0 ; i.e., RADAMS gradually decreases $m \in \{0, 1, 2, 3\}$, the number of de-emphasized alerts. As shown in the lower figure, the resilience margin increases monotonously with the cost. The optimal strategy for alerts of high criticality yields a larger resilience margin than the one for low criticality.

Remark 6 (Tradeoff of Monitoring and Inspection). *The results show that the optimal strategy strikes a balance between real-time monitoring a large number of alerts and inspecting selected alerts with high quality. Moreover, the optimal strategy is resilient for a large range of cost values ([\\$0, \\$1000]). If the cost is high and the alert is of low*

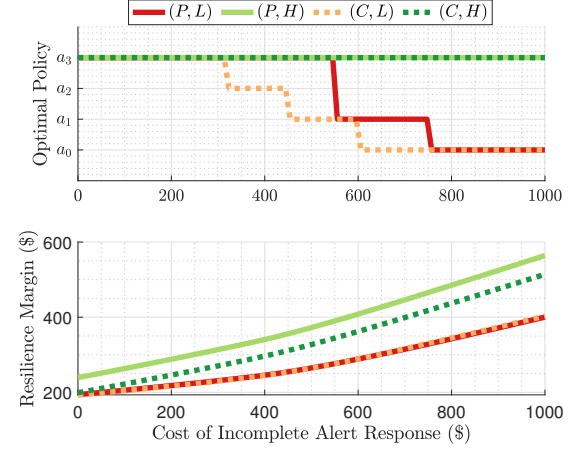


Fig. 5: The optimal AM strategy and the risk vs. the cost of an incomplete alert response under category label $(s_{SO,P}, s_{CR,L})$, $(s_{SO,P}, s_{CR,H})$, $(s_{SO,C}, s_{CR,L})$, and $(s_{SO,C}, s_{CR,H})$ in solid red, solid green, dashed yellow, and dashed green, respectively.

(resp. high) criticality, then the optimal strategy encourages monitoring (resp. inspecting) by choosing a small (resp. large) m . However, when the cost of an incomplete alert response is relatively low, the optimal strategy is a_4 for all alerts as the high-quality inspection outweighs the high-quantity monitoring.

3) *Arrival Frequency of IDoS Attacks:* As stated in Section III-A, feint attacks with the goal of triggering alerts require fewer resources to craft. Thus, we let $\hat{c}_{RE} = \$0.04$ and $\hat{c}_{FE} \in (0, \hat{c}_{RE})$ denote the cost to generate a real attack and a feint, respectively. With \hat{c}_{RE} and \hat{c}_{FE} , we can compute the attack cost of feint and real attacks per work shift of 24 hours. Let ρ be the scaling factor for the arrival frequency and in Section VII-B3, the average inter-arrival time is $\hat{\mu}(\theta^k, \theta^{k+1}) = \rho \mu(\theta^k, \theta^{k+1})$, $\forall \theta^k, \theta^{k+1} \in \Theta$. We investigate how the scale factor $\rho \in (0, 2.5]$ affects the IDoS risk and the attack cost in Fig. 6. As ρ decreases, the attacker generates feint and real attacks at a higher frequency. Then, the risks under both the optimal and the default strategies increase. However, the optimal AM strategy can reduce the increase rate for a large range of $\rho \in [0.5, 2]$.

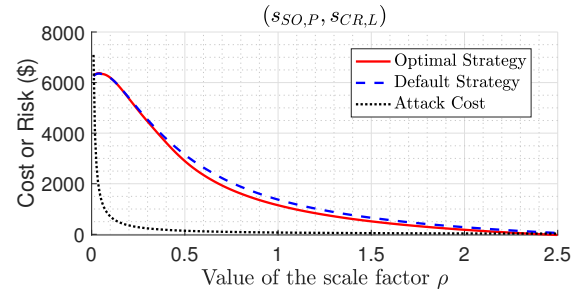


Fig. 6: IDoS risk vs. ρ under the optimal and the default AM strategies in solid red and dashed blue, respectively. The black line represents the attack cost per work shift of 24 hours.

Remark 7 (Attacker's Dilemma). *From the attacker's perspective, although increasing the attack frequency can induce*

a high risk to the organization and the attacker can gain from it, the frequency increase also increases the attack cost exponentially as shown by the dotted black line in Fig. 6. Thus, the attacker has to strike a balance between the attack cost and the attack gain (represented by the IDoS risk). Moreover, attackers with a limited budget are not capable to choose small values of ρ (i.e., high attack frequencies).

4) *Percentage of Feint and Real Attacks:* Consider the case where κ_{AT} independently generates feints and real attacks with probability η_{FE} and $\eta_{RE} = 1 - \eta_{FE}$, respectively. We consider the case where the attacker has a limited budget $\hat{c}_{max} = \$270$ per work shift (i.e., 86400s) and generates feint and real attacks at the same rate $\hat{\beta}$, i.e., $\beta(\theta^k, \theta^{k+1}) = \hat{\beta}, \forall \theta^k, \theta^{k+1} \in \Theta$. Consider the attack cost in Section VII-B3, the attacker has the following budget constraint, i.e.,

$$86400 \cdot \hat{\beta} \cdot (\eta_{FE} \hat{c}_{FE} + \eta_{RE} \hat{c}_{RE}) \leq \hat{c}_{max}. \quad (12)$$

The budget constraint results in the following tradeoff. If the attacker chooses to increase the probability of real attack η_{RE} , then he has to reduce the arrival frequency $\hat{\beta}$ of feint and real attacks. We investigate how the probability of feints affects the IDoS risk in Fig. 7 under the optimal and the default AM strategies in red and blue, respectively. The feints are of low and high costs in Fig. 7a and 7b, respectively.

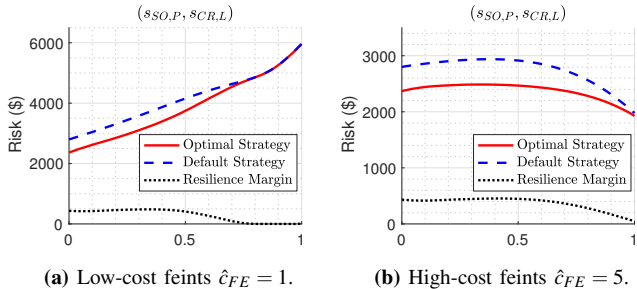


Fig. 7: IDoS risk vs. $\eta_{FE} \in [0, 1]$ under the optimal and the default AM strategies in red and blue, respectively. The black line represents the resilience margin.

As shown in Fig. 7a, when the feints are of low cost, i.e., $\hat{c}_{FE} = \hat{c}_{RE}/10$, generating feints with a higher probability monotonously increases the IDoS risks for both AM strategies. When the probability of feints is higher than 80%, the resilience margin is zero; i.e., the optimal and the default AM strategies both induce high risks. However, as the probability of feint decreases, the resilience margin increases to around \$500; i.e., the default strategy can moderately reduce the risk but the optimal strategy can excessively reduce the risk.

Remark 8 (Half-Truth Attack for High-Cost Feints). As shown in Fig. 7b, when the feints are of high cost, i.e., $\hat{c}_{FE} = \hat{c}_{RE}/2$, then the optimal attack strategy is to deceive with half-truth, i.e., generating feint and real attacks with approximately equal probability to induce the maximum IDoS risk. As the probability of feints decreases from $\eta_{FE} = 1$, the risk increases significantly under the default AM strategy but moderately under the optimal one.

The figures in Fig. 7 show that the optimal attack strategy under the budget constraint (12) needs to adapt to the cost of

feint generation. Regardless of the attack strategy, the optimal AM strategy can reduce the risk and achieve a positive resilient margin for all category labels $(s_{SO,i}, s_{CR,j}), i \in \{P, C\}, j \in \{L, H\}$. Moreover, higher feint generation cost reduces the arrival frequency of IDoS attacks due to (12). Thus, comparing to Fig. 7a, the risk in Fig. 7b is lower for the same η_{FE} under the optimal or the default AM strategies, especially when η_{FE} is close to 1.

5) *The Operator’s Attention Capacity:* We consider the following attention function $f_{LOE} \circ f_{SL}$ with a constant attention threshold, i.e., $\bar{n}(y_{EL}, s^k) = \bar{n}_0, \forall y_{EL}, s^k \in \mathcal{S}$. Consider the following trapezoid attention function. If $n^t \leq \bar{n}_0$, the LOE $\omega^t = 1$; i.e., the operator can retain the high LOE when the number of distractions is less than the attention threshold \bar{n}_0 . If $n^t > \bar{n}_0$, the LOE ω^t gradually decreases as n^t increases. Then, a larger value of \bar{n}_0 indicates a high attention capacity. We investigate how the value of \bar{n}_0 affects the risk in Fig. 8.

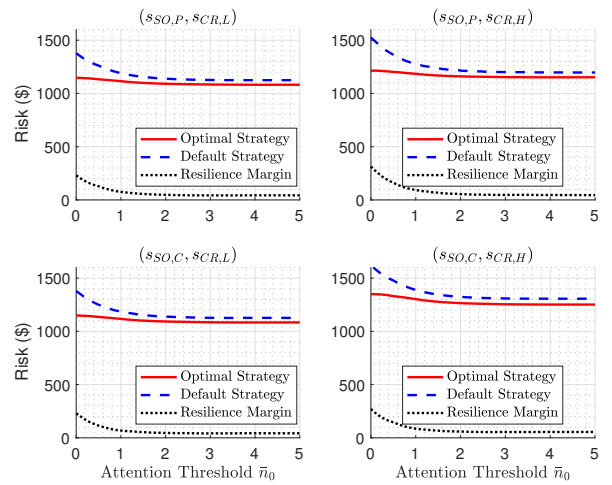


Fig. 8: Risk vs. attention threshold under the optimal and the default AM strategies in red and blue, respectively. The black dotted line represents the resilience margin.

As the operator’s attention capacity increases, the risks under the optimal and the default AM strategies decrease for all category labels. The resilience margin decreases from around \$200 to \$50 as \bar{n}_0 increases from 0 to 2 and then maintains the value of around \$50. Thus, the optimal strategy suits operators with a large range of attention capacity, especially for the ones with limited attention capacity.

VIII. CONCLUSION

Attentional human vulnerabilities exploited by attackers lead to a new class of proactive attacks called the Informational Denial-of-Service (IDoS) attacks. IDoS attacks generate a large number of feint attacks on purpose to deplete the limited human attention resources and exacerbate the alert fatigue problem. In this work, we have formally defined IDoS attacks as a sequence of feint and real attacks of heterogeneous targets, which can be characterized by the Markov renewal process. We have abstracted the alert generation and triage processes as a revelation probability to establish a stochastic relationship

between the IDoS attack's hidden types and targets and the associated alert's observable category labels. We have explicitly incorporated human factors (e.g., levels of expertise, stress, and efficiency) and empirical results (e.g., the Yerkes–Dodson law and the sunk cost fallacy) to model the operators' attention dynamics and the processes of alert monitoring, inspection, and response in real time. Based on the system-scientific human attention and alert response model, we have developed a Resilient and Adaptive Data-driven alert and Attention Management Strategy (RADAMS) to assist human operators in combating IDoS attacks. We have proposed a Reinforcement Learning (RL)-based algorithm to obtain the optimal assistive strategy according to the costs of the operator's alert responses in real time.

Through theoretical analysis, we have observed the *Product Principle of Attention* (PPoA), the fundamental limits of Attentional Deficiency Level (ADL) and risk, and tradeoff among the ADL, the reward of alert attention, and the impact of alert inattention. Through the experimental results, we have corroborated the *effectiveness, adaptiveness, robustness, and resilience* of the proposed assistive strategies. First, the optimal AM strategy outperforms the default strategy and can effectively reduce the IDoS risk by as much as 20%. Second, the strategy adapts to different category labels to strike a balance of monitoring and inspections. Third, the optimal AM strategy is robust to deviations. We can apply sub-optimal strategies at some category labels without significantly increasing the IDoS risk. Finally, the optimal AM strategy is resilient to a large variations of costs, attack frequencies, and human attention capacities.

REFERENCES

- [1] L. Huang and Q. Zhu, "Combating informational denial-of-service (IDoS) attacks: Modeling and mitigation of attentional human vulnerability," in *International Conference on Decision and Game Theory for Security*. Springer, 2021.
- [2] G. Bassett, C. D. Hylander, P. Langlois, A. Pinto, and S. Widup, "Data breach investigations report," Verizon DBIR Team, Tech. Rep., 2021.
- [3] Tessian, "The psychology of human error," Tech. Rep., 2020.
- [4] B. Hitzel. (2019) The art of cyber war and cyber battle: Deception operations. <https://www.networkdefenseblog.com/post/art-of-cyber-war-deception>.
- [5] R. M. Yerkes, J. D. Dodson *et al.*, "The relation of strength of stimulus to rapidity of habit-formation," *Punishment: Issues and experiments*, pp. 27–41, 1908.
- [6] H. R. Arkes and C. Blumer, "The psychology of sunk cost," *Organizational behavior and human decision processes*, vol. 35, no. 1, pp. 124–140, 1985.
- [7] L. Huang and Q. Zhu, "A dynamic games approach to proactive defense strategies against advanced persistent threats in cyber-physical systems," *Computers & Security*, vol. 89, p. 101660, 2020.
- [8] —, "Adaptive honeypot engagement through reinforcement learning of semi-markov decision processes," in *International Conference on Decision and Game Theory for Security*. Springer, 2019, pp. 196–216.
- [9] —, "Farsighted risk mitigation of lateral movement using dynamic cognitive honeypots," in *International Conference on Decision and Game Theory for Security*. Springer, 2020, pp. 125–146.
- [10] S. Jajodia, A. K. Ghosh, V. Swarup, C. Wang, and X. S. Wang, *Moving target defense: creating asymmetric uncertainty for cyber threats*. Springer Science & Business Media, 2011, vol. 54.
- [11] W. Casey, J. A. Morales, E. Wright, Q. Zhu, and B. Mishra, "Compliance signaling games: toward modeling the deterrence of insider threats," *Computational and Mathematical Organization Theory*, vol. 22, no. 3, pp. 318–349, 2016.
- [12] D. Liu, X. Wang, and L. J. Camp, "Mitigating inadvertent insider threats with incentives," in *International Conference on Financial Cryptography and Data Security*. Springer, 2009, pp. 1–16.
- [13] L. Huang and Q. Zhu, "Duplicity games for deception design with an application to insider threat mitigation," *IEEE Transactions on Information Forensics and Security*, vol. 16, pp. 4843–4856, 2021.
- [14] G. Spathoulas and S. Katsikas, "Reducing false positives in intrusion detection systems," *Comput & Secur*, vol. 29, no. 1, pp. 35–44, 2010.
- [15] H. Elshoush and I. Osman, "Reducing false positives through fuzzy alert correlation in collaborative intelligent intrusion detection systems—a review," in *IEEE Int. Conf. Fuzzy Syst.* IEEE, 2010, pp. 1–8.
- [16] K. Goeschel, "Reducing false positives in intrusion detection systems using data-mining techniques utilizing support vector machines, decision trees, and naive bayes for off-line analysis," in *SoutheastCon 2016*. IEEE, 2016, pp. 1–6.
- [17] S. Salah, G. Maciá-Fernández, and J. E. Díaz-Verdejo, "A model-based survey of alert correlation techniques," *Computer Networks*, vol. 57, no. 5, pp. 1289–1317, 2013.
- [18] A. Shah, R. Ganesan, S. Jajodia, and H. Cam, "A two-step approach to optimal selection of alerts for investigation in a csoc," *IEEE Trans. Inf. Forensics Secur*, vol. 14, no. 7, pp. 1857–1870, 2019.
- [19] E. A. Newcomb, R. J. Hammell, and S. Hutchinson, "Effective prioritization of network intrusion alerts to enhance situational awareness," in *2016 IEEE Conference on Intelligence and Security Informatics (ISI)*. IEEE, 2016, pp. 73–78.
- [20] S. McElwee, J. Heaton, J. Fraley, and J. Cannady, "Deep learning for prioritizing and responding to intrusion detection alerts," in *IEEE Military Communications Conference*. IEEE, 2017, pp. 1–5.
- [21] R. Ganesan, S. Jajodia, A. Shah, and H. Cam, "Dynamic scheduling of cybersecurity analysts for minimizing risk using reinforcement learning," *ACM Transactions on Intelligent Systems and Technology (TIST)*, vol. 8, no. 1, pp. 1–21, 2016.
- [22] I. Corona, G. Giacinto, and F. Roli, "Adversarial attacks against intrusion detection systems: Taxonomy, solutions and open issues," *Information Sciences*, vol. 239, pp. 201–225, 2013.
- [23] D. Mutz, G. Vigna, and R. Kemmerer, "An experience developing an ids stimulator for the black-box testing of network intrusion detection systems," in *19th Annual Computer Security Applications Conference, 2003. Proceedings*. IEEE, 2003, pp. 374–383.
- [24] S. Patton, W. Yurcik, and D. Doss, "An achilles' heel in signature-based ids: Squealing false positives in snort," in *Proceedings of RAID*, vol. 2001. Citeseer, 2001.
- [25] M. Roesch *et al.*, "Snort: Lightweight intrusion detection for networks." in *Lisa*, vol. 99, no. 1, 1999, pp. 229–238.
- [26] Z. Wang, H. Zhu, and L. Sun, "Social engineering in cybersecurity: Effect mechanisms, human vulnerabilities and attack methods," *IEEE Access*, vol. 9, pp. 11895–11910, 2021.
- [27] S. Miserendino, C. Maynard, and J. Davis, "Threatvectors: Contextual workflows and visualizations for rapid cyber event triage," in *2017 International Conference On Cyber Incident Response, Coordination, Containment & Control (Cyber Incident)*. IEEE, 2017, pp. 1–8.
- [28] L. Franklin, M. Pirrung, L. Blaha, M. Dowling, and M. Feng, "Toward a visualization-supported workflow for cyber alert management using threat models and human-centered design," in *2017 IEEE Symposium on Visualization for Cyber Security (VizSec)*. IEEE, 2017, pp. 1–8.
- [29] L. Huang and Q. Zhu, "Inadvert: An interactive and adaptive counter-deception platform for attention enhancement and phishing prevention," *arXiv preprint arXiv:2106.06907*, 2021.
- [30] S. C. Sundaramurthy, A. G. Bardas, J. Case, X. Ou, M. Wesch, J. McHugh, and S. R. Rajagopalan, "A human capital model for mitigating security analyst burnout," in *Eleventh Symposium On Usable Privacy and Security (SOUPS) 2015*, 2015, pp. 347–359.
- [31] C. Zimmerman, "Ten strategies of a world-class cybersecurity operations center," *The MITRE Corporation*, 2014.
- [32] R. D. Yates, Y. Sun, D. R. Brown, S. K. Kaul, E. H. Modiano, and S. Ulukus, "Age of information: An introduction and survey," *IEEE J. Sel. Areas Commun.*, vol. 39, pp. 1183–1210, 2021.
- [33] J. S. Ancker, A. Edwards, S. Nosal, D. Hauser, E. Mauer, and R. Kaushal, "Effects of workload, work complexity, and repeated alerts on alert fatigue in a clinical decision support system," *BMC medical informatics and decision making*, vol. 17, no. 1, pp. 1–9, 2017.
- [34] D. P. Bertsekas and J. N. Tsitsiklis, *Neuro-dynamic programming*. Athena Scientific, 1996.
- [35] A. Shah, R. Ganesan, S. Jajodia, and H. Cam, "Understanding tradeoffs between throughput, quality, and cost of alert analysis in a csoc," *IEEE Transactions on Information Forensics and Security*, vol. 14, no. 5, pp. 1155–1170, 2019.